

Tailored saturation functions and its application to liquid uptake processes in fibrous composite reinforcements

Volume 52: 1–15

© The Author(s) 2022

Article reuse guidelines:

sagepub.com/journals-permissions

DOI: 10.1177/15280837221118093

journals.sagepub.com/home/jit

László M Vas¹, Zoltán Gombos², Veronika Nagy³ and Marianna Halász⁴ 

Abstract

Saturation processes occur in almost every theoretical and practical field, e.g. liquid uptake within fibrous composite reinforcements. These processes require appropriate mathematical functions to model them and use them for design purposes. This includes assessing the saturation level, especially in microfluidic processes of fibrous composite reinforcements. This paper proposes a mathematical approach that uses a simple and well-known saturation function with modification through variable transformations and/or linear combinations. When the initial asymptotic behaviour is numerically known, this modified function provides a tailored and robust approximation of the measured saturation process and makes it possible to assess the asymptotic saturation level as well. A saturation function based on micro-tensiometer measurements and a simple exponential function was applied to validate this method. The mathematical approach was validated by

¹Department of Polymer Engineering, Budapest University of Technology and Economics, Faculty of Mechanical Engineering, Budapest, Hungary

²Exeter Advanced Technologies, College of Engineering, Mathematics, and Physical Sciences, University of Exeter, Exeter, UK

³MOL Magyar Olaj- és Gázipari Nyrt, Tiszaújváros, Hungary

⁴Sándor Rejtő Faculty of Light Industry and Environmental Protection Engineering, Institute for Industrial Product Design, Óbuda University

Corresponding author:

Marianna Halász, Óbuda University, Sándor Rejtő Faculty of Light Industry and Environmental Protection Engineering, Institute for Industrial Product Design, Bécsi út 96/B, Budapest H-1034, Hungary.

Email: halasz.marianna@rkk.uni-obuda.hu



Creative Commons Non Commercial CC BY-NC: This article is distributed under the terms of the Creative Commons Attribution-NonCommercial 4.0 License (<https://creativecommons.org/licenses/by-nc/4.0/>) which permits non-commercial use,

reproduction and distribution of the work without further permission provided the original work is attributed as specified on the SAGE and Open Access pages (<https://us.sagepub.com/en-us/nam/open-access-at-sage>).

test results based on distilled water uptake in polyester yarns and unsaturated polyester (UP) resin absorption within fibreglass chopped strand mats. In both cases, a good correlation was found between the experimental results and the applied mathematical approach, where the determination coefficients were higher than 0.989.

Keywords

saturation process, mathematical function fitting, liquid uptake, composite reinforcements, polyester yarns, fibreglass chopped strand mats

Introduction

Computer-based modelling methods make it possible for engineers to design structural parts made from polymers or polymer composites that are more reliable and have an extended lifespan. However, they require relevant functional data and a mathematical approach to describe the effect of the structural, mechanical, and environmental parameters on the material properties.¹⁻⁵ These functions often have limitations in describing the processes up to the saturation level.^{1,5-9} In general, saturation is a process that tends to reach the equilibrium of a system or the maximum permeability of a channel. This often occurs in mass transport such as gas, liquid, or other medium transfer.

One of the most frequent saturation processes in polymer materials science and engineering is the liquid uptake of structural materials, such as liquid treatment of polymers and/or resin uptake during impregnating fibres, such as during the manufacture of fibre reinforced polymer composites.⁸ In general, some polymers and porous or fibrous materials can uptake liquid or moisture by capillary action through chains of pores, micro-cracks^{1,3,4} and/or diffusion of liquid or vapour molecules into their structure.^{1,10,11} In practice, it is important to know not only the initial rate of the liquid uptake process but also the degree of saturation at the specified time and the saturation level. The former can usually be investigated with a micro-tensiometer,¹² while the assessment of the latter needs a suitable mathematical model where time-consuming observation is not feasible.

This paper proposes a method of tailored, robust, and flexible saturation functions as a numerical approximation using different types of measured saturation processes based on a well-known saturation function with modification through variable transformations and/or linear combination. To demonstrate the applicability of the proposed method, liquid uptake measurements were performed on polyester yarn with water as well as two different types of fibreglass chopped strand mats with unsaturated polyester (UP) resin, and then the results were analysed. The generated saturation function was applied to fit the liquid uptake measurements based on the simple exponential function and the Lucas-Washburn equation¹²⁻¹⁴ as well as on K12 micro-tensiometer measurements.¹² This applied function has just a few parameters and behaves as a robust expression fitting the data obtained from measurements. This method can provide parameters that can characterise both the initial and the asymptotic behaviours, including the saturation value of the liquid uptake.

Theoretical considerations

Let $S(x)$ be a saturation function (SF)^{1,5-8,12-14} if it is continuous, increasing monotonic, and bounded by finite real values $S(0) = S_0$ and S_∞ that is ($0 \leq x$)

$$S_0 \leq S(x) = S_0 + (S_\infty - S_0)s(x) \leq S_\infty \tag{1}$$

$$S(x) \rightarrow S_\infty, \quad x \rightarrow \infty \tag{2}$$

where S_∞ is the saturation value and $s(x)$ is the normalised saturation function (NSF)

$$s(x) = \frac{S(x) - S_0}{S_\infty - S_0} \rightarrow \begin{cases} 0, & x \rightarrow 0 \\ 1, & x \rightarrow \infty \end{cases} \tag{3}$$

The assumption that $S_0 = 0$ is not against the generality; therefore, $S(x) = S_\infty \cdot s(x)$ can be considered. In most cases, the initial behavior of a given saturation process can be determined by short-term measurements. Hence, let $s_0(x)$ be the measured initial asymptote of $s(x)$, that is

$$\frac{S(x)}{S_\infty s_0(x)} = \frac{s(x)}{s_0(x)} \xrightarrow{x \rightarrow 0} 1 \tag{4}$$

where $s_0(x)$ is assumed to be a strictly increasing monotonic function, but it is not bounded

$$s(x) \leq s_0(x) \xrightarrow{x \rightarrow \infty} \infty \tag{5}$$

The aim of the short-term measurements is to describe the quasi-static long-term saturation process and assess the saturation value. To achieve that, a suitable and robust mathematical function must be found that can be used to fit the measurements, and its initial asymptote $s_0(x)$ is also known function. In general, in all scientific engineering fields, a simple hyperbolic or exponential function, $w(x)$, can be found that is used to describe saturation processes. Fitting $w(x)$ can often be performed only with a significant error that makes assessing the saturation value highly uncertain. In this case, the subsequent formula-construction method based on variable transformations is proposed to use.

It is obvious that if $w(z)$ is an NSF, then the next variable transformed functions are NSF as well ($0 \leq z, 0 < n$)

$$f(z) = w(z^n), \quad g(z) = w^n(z), \quad h(z) = 1 - (1 - w(z))^n \tag{6}$$

Regarding equation (5), this is also true if $z = a s_0(x)$ ($a > 0$) and we combine some transformations by equation (6) ($0 \leq z, 0 < m, n, a$)

$$v(z) = w^n(z^m) = w^n(a^m s_0^m(x)) =: \widehat{s}(x) \tag{7}$$

Here, exponents m and n are to be chosen so that the initial asymptote of $\widehat{s}(x)$ equals the measured $s_0(x)$. Supposing $w(z)$ can be expanded into the Taylor series about $z = 0$ ¹⁵ the initial asymptote is a simple power function since $w(0) = 0$. Let this power function be cz^k ($c, k > 0$). Using this for equation (7) yields

$$\widehat{s}(x) = w^n(s_0^m(x)) \sim [c^m a^{km} s_0^{km}(x)]^n = c^{mn} a^{kmn} s_0^{kmn}(x) = s_0(x), \quad x \rightarrow 0 \quad (8)$$

The equation on the right side of equation (8) stands if $n = 1/km$ and $a = c^{-1/k}$ providing that the initial asymptote of $\widehat{s}(x)$ is $s_0(x)$. In addition, the appropriate choice of exponent m may give a good fitting to the measurements and enables a suitable assessment of S_∞ saturation value.

Considering the basic NSF, $w(z)$, in different scientific fields, it is often an exponential^{1,8} or a hyperbolic⁵ function. Since it is well known from the mathematical analysis that there is a convergent hyperbolic function series that tends to an exponential limit function¹⁵ the saturation functions of hyperbolic and exponential types can be treated together

$$q_r(z) = \frac{1}{[1 + rz]^{1/r}} \xrightarrow{r \rightarrow 0} e^{-z} =: q(z) \quad (9)$$

It can be noted that the basic NSF may also be a simple logistic function that is often used for describing development or growth processes in biology or economy.⁷

Since $w_r(z) = 1 - q_r(z)$ and $w(z) = 1 - q(z)$ meet the requirements of an NSF, they can be applied to construct a similar NSF series that has got the measured initial asymptote, $s_0(x) = z$, as well ($a = 0$)

$$\widehat{s}_r(x) = \left[1 - \frac{1}{[1 + rs_0^n(x)]^{1/r}} \right]^{\frac{1}{n}} = \left[1 - \frac{1}{[1 + rz^n]^{1/r}} \right]^{\frac{1}{n}} \xrightarrow{r \rightarrow 0} [1 - e^{-z^n(x)}]^{\frac{1}{n}} = [1 - e^{-s_0^n(x)}]^{\frac{1}{n}} = \widehat{s}(x) \quad (10)$$

Any of the robust saturation functions $\widehat{s}_r(x)$ and $\widehat{s}(x)$ by equation (10) can be used for fitting measurements where the free fitting parameters are dimensionless exponents (r, n) or just n .

To make the approximation more accurate, the construction of a saturation function by the convex linear combination of appropriate upper (s_U) and lower (s_L) bounds of the saturation function defined, for example, by equation (10) with suitable exponents, r and n , can be used

$$s_L(z) \leq s(x) \leq s_U(z) \quad (11)$$

$$s(x) = \alpha s_L(z) + (1 - \alpha) s_U(z) \quad (12)$$

where $0 \leq \alpha \leq 1$ is the weighting parameter. Note that α may be a weighting function, for example $\alpha(x) = \exp(-bx)$ ($b > 0$) is an exponential weight that is often used in statistics.

Based on the considerations above, three different methods may be proposed to obtain a robust saturation function suitable for fitting to the measured saturation process with good correlation and assessing the saturation value at a steady-state:

1. Construct a normalised saturation function based on a previously known simple saturation function – for example, derived from a simple model – and a measured normalised saturation process applying equation (6) to modifying. Equation (12) can be used in case of a more accurate approximation.
2. Construct a normalised saturation function based on a measured saturation process and its initial asymptote function identified from measurement (performed by e.g. a micro-tensiometer in case of a liquid uptake) applying equation (10).
3. Direct application of the saturation functions by equation (10) to fit where $s_0(x)$ is considered as a simple power function like $s_0(x) = cx^m$.

Unknown parameters such as saturation value S_∞ and exponents n and r or, if required, those (c and m) for the initial asymptote $s_0(x)$ can be determined from fitting.

Application to liquid uptake processes in fibrous materials

In general, liquid uptake in a fibrous material is a mass transport process that may occur via capillary and diffusion actions.¹ The former takes place as fluid flow through capillaries between the fibres like wicking. The latter means the results of absorbing liquid molecules enabled by Brownian motion.

To validate the construction method proposed in *Theoretical Considerations*, a liquid uptake process was selected for analysis and approximation where construction methods (1) and (2) were applied. Firstly, an approximate explicit solution of the Lucas-Washburn equation was derived as a simple saturation function and its initial asymptote that can be identified by a micro-tensiometer. Finally, equation (10) was applied to construct a tailored saturation function that describes both the capillary and the diffusive liquid uptake. It is presented in this study that the robust mathematical formula constructed to describe the measured liquid uptake process in different materials corresponds to equation (10).

Capillary liquid uptake

To describe the liquid uptake behaviour of filter papers, R. Lucas¹³ derived a differential equation for the time-dependent rise of liquids in a single straight vertical capillary tube of diameter $d = 2r$ with open ends, where one end was in contact with the surface of a Newtonian liquid. Later, E.W. Washburn¹⁴ obtained a similar but more general

differential equation, where he considered a capillary of arbitrary shape with either an open or closed non-contacting end, including horizontal and vertical capillaries, as extreme cases. In the case of a straight but oblique capillary, Washburn's nonlinear differential equation formulated for the time (t) dependent liquid mass ($m = \rho\pi r^2 l$) proportional to the length (l) of liquid penetration and the related constants (a [g^2/s], b [g/s]) are given by equation (13)¹⁴

$$\frac{dm}{dt} = \frac{a - bm}{m}, a = \rho^2 \pi^2 \frac{2r\gamma \cos\theta}{8\eta} (r^4 - 4\beta r^3), b = \frac{\rho^2 g \pi \sin\psi}{8\eta} (r^4 - 4\beta r^3) \quad (13)$$

where $0^\circ \leq \psi \leq 90^\circ$ is the slope angle of the capillary and $L > 0$ is the total length of the capillary ($l \leq L$). The constant parameters γ , η and ρ are the surface tension, viscosity, and density of the liquid, respectively, g is the gravitational acceleration ($g = 9.81 \text{ m/s}^2$), $0 \leq \theta < 90^\circ$ is the contact angle between the wetting liquid and the capillary surface, and $\beta \geq 0$ is the coefficient of slip (or slip length), which is assumed to be zero for wetting materials.¹⁴

Equation (13) is usually called the Lucas-Washburn equation, the parameters (a , b) of which can be obtained if $\beta = 0$, $h_C = 0$, and $\psi = 90^\circ$. Equation (13) describes an equilibrium process; hence its solution must tend to the saturation level value (m_∞) with time, consequently, the derivative tends to 0 when $t \rightarrow \infty$

$$m_\infty = \frac{a}{b} = \frac{2\pi\gamma \cos\theta}{g \sin\psi} r = c \cdot r, \quad c = \frac{2\pi\gamma \cos\theta}{g \sin\psi} \quad (14)$$

where c is a proportionality constant defined by equation (14) and characterises the liquid/fiber system. When $m(t) \ll m_\infty$, and $a \gg bm$, as well as $m(0) = 0$, the integration of equation (13) leads to a simple explicit solution, $m_0(t)$, which is also called Lucas-Washburn equation¹² and corresponds to $s_\theta(x)$ function by equation (5)

$$m(t) \approx m_0(t) = \sqrt{2at} = K\sqrt{t}, \quad t \rightarrow 0 \quad (15)$$

The constant K defined by equation (15) characterises the initial uptake rate or intensity, and it is a basic function that is used for evaluating micro-tensiometer measurements.¹²

Equation (13) is a separable differential equation that can be solved by simple integration. Assuming $\psi > 0^\circ$ and rearranging equation (13), its integration under initial condition $m(0) = 0$ yields the general (implicit) solution of the Lucas-Washburn differential equation

$$bt = -\frac{a}{b} \ln\left(1 - \frac{b}{a}m\right) - m = m_\infty \left[-\ln\left(1 - \frac{m}{m_\infty}\right) - \frac{m}{m_\infty} \right] =: m_\infty G\left(\frac{m}{m_\infty}\right) \quad (16)$$

This solution by equation (16) is invertible, but its inverse, the explicit form, cannot be expressed with basic functions. After normalising equation (16) with m_∞ , one can extend the logarithmic expression in a power series as follows

$$\frac{bt}{m_\infty} = \ln \frac{1}{1 - m(t)/m_\infty} - \frac{m(t)}{m_\infty} = \frac{1}{2} \left(\frac{m}{m_\infty}\right)^2 + \frac{1}{3} \left(\frac{m}{m_\infty}\right)^3 + \frac{1}{4} \left(\frac{m}{m_\infty}\right)^4 + \dots \quad (17)$$

The first term of the series on the right side gives an explicit approximate solution, with which the initial part of the measured process can be estimated, and it is equivalent to equation (12). A simple upper implicit estimation by equation (18), convertible into an explicit form, can be obtained from the implicit solution with the use of equation (17)

$$\frac{1}{2} \left(\frac{m}{m_\infty}\right)^2 \leq \frac{bt}{m_\infty} = \ln \frac{1}{1 - \frac{m}{m_\infty}} + \ln e^{-\frac{m}{m_\infty}} = \ln \frac{1}{\left(1 - \frac{m}{m_\infty}\right) e^{\frac{m}{m_\infty}}} \leq \ln \frac{1}{1 - (m/m_\infty)^2} \quad (18)$$

The normalised explicit forms of the upper and lower estimations in equation (18) are as follows

$$\begin{aligned} \left[1 - \exp\left(-\frac{bt}{m_\infty}\right)\right]^{1/2} &= \left[1 - \exp\left(-\left(\frac{1}{\sqrt{2}} \sqrt{\frac{2bt}{m_\infty}}\right)^2\right)\right]^{1/2} \leq \frac{m(t)}{m_\infty} \leq \min\left\{\sqrt{\frac{2bt}{m_\infty}}, 1\right\} \\ &\leq \sqrt{\frac{2bt}{m_\infty}} = \frac{m_0(t)}{m_\infty} \end{aligned} \quad (19)$$

The lower explicit estimation, according to equation (19), is asymptotically correct both when $t \rightarrow \infty$ and when $t \rightarrow 0$ and is formally the special case of the general formula equation (10). The explicit upper estimation is correct just regarding the initial asymptote. A refined estimation needs to increase the lower bound in equation (19) while staying below the upper bound and retaining that as an initial asymptote. All that can be obtained by using the transformation according to equation (10) that provided the general normalised form of the explicit approximate solution for liquid uptake and its initial asymptote ($t \sim 0$) given by

$$m(t) \approx m_\infty \left[1 - e^{-\left(\frac{m_0(t)}{m_\infty}\right)^n}\right]^{\frac{1}{n}} \rightarrow \begin{cases} \rightarrow 1, & (t \rightarrow \infty) \\ \sim m_0(t) = K\sqrt{t} = \sqrt{2at}, & (t \rightarrow 0) \end{cases} \quad (20)$$

where n is a positive constant. Equation (20) is a kind of generalised form of equation (19) (left side) containing the initial asymptote, $m_0(t)$, defined by equation (15), and it is identical to equation (10).

Equation (20) is a rather general three-parameter (K, m_∞, n) formula for the description of time-dependent saturation processes. In practice, it is enough to know the initial absorption behaviour, $m_0(t)$, given by constant K (or b or a), and the equilibrium value, m_∞ . The former can be estimated, e.g. from micro-tensiometer measurement, while the latter (or both) and the shape parameter (exponent n) can be determined by fitting data obtained from a relatively short measurement suitable for assessment.

It should be noted that although the Lucas-Washburn equation is not a new approach, yet it has been widely utilised nowadays when porous or fibrous materials are studied and modelled.^{16–20}

Diffusive liquid uptake

Nanofluidic liquid uptake through diffusion can be described with Fick's second law¹ The related transport equation is a partial differential equation of second-order. In general, its solution has got the form of an infinite series. For one-dimensional diffusion into a thin plate composed of thin layers of $h = 2\delta$ thickness, Carter and Kibler²¹ determined a solution for the fractional increase in the mass of the sample in the time interval $(0, t)$, which is given by equation (21)

$$P(t) = \frac{m(t)}{m_0} = P_e \left[1 - \frac{8}{\pi^2} \sum_{n=0}^{\infty} \frac{1}{(2n+1)^2} e^{-(2n+1)^2 kt} \right] = \begin{cases} \sim K_e \sqrt{t}, & t \rightarrow 0 \\ \rightarrow P_e = \frac{m_{\infty}}{m_0} & t \rightarrow \infty \end{cases} \quad (21)$$

where $P(0) = 0$ and P_e is the saturation level that is the mass increase ratio related to the dry mass m_0 , and constant k depends on the diffusion coefficient, and the thickness K_e is a constant determining the initial rate and the initial asymptote that is formally identical with equation (15). It should be noted that Belhadj et al.²² recently applied a similar solution for studying moisture concentration in graphite fiber-reinforced polymer composites.

Application to joint capillary and diffusive liquid uptake

In some cases, liquid uptake is the result of capillary imbibition and a diffusion process e.g. a specimen immersed in liquid. Equation (20) can be applied to the sum of these processes as well. Consider equations (15) and (21), so the total liquid uptake of the sample, including both the active capillaries (number and radius of them are N and r_i , $i = 1, \dots, N$, respectively) and the diffusive process is given by equation (22)

$$m(t) = m_C(t) + m_D(t) = \begin{cases} \sim (K_C + K_D) \sqrt{t} = K \sqrt{t} = m_0(t), & t \rightarrow 0 \\ \rightarrow m_{\infty} = m_{C\infty} + m_{D\infty} & t \rightarrow \infty \end{cases} \quad (22)$$

where K_C and K_D , $m_{C\infty}$ and $m_{D\infty}$ are constants characterising the initial rates and the saturation of capillary (C) and diffusive (D) liquid uptake, respectively. Hence, diffusion-based or mixed liquid uptake can also be modelled with a capillary system.

Materials and measurement methods

Experimental data from our previous research^{23,24} was used to validate the saturation function construction method and the liquid uptake functions. These results were obtained

by testing water and resin uptake in fibrous structures such as polyester yarns and fibreglass chopped strand mats, respectively. Initial and global explicit approximate functions according to equations (15) and (20) were applied to fit the measured liquid uptake processes.

Materials

The tested yarn samples were polyester (PET) ring-spun staple yarns produced by Du Pont de Nemours Inc. with the same yarn count or, in another term, linear density ($q = 19.67$ tex) and twist level (1000 tpm).²³ The fibre length of the yarns was the same, but their cross-sections differed. Round and scalloped oval (Figure 1) fibre shapes were applied in this study, while their mean area-equivalent diameter was $14.14 \mu\text{m}$ and $13.69 \mu\text{m}$, respectively.²³

The fibreglass chopped strand mats (CSMs) that were evaluated in this study [24] were produced by Johns Manville Ltd. (JM) (Figure 2). The nominal density of the E-type glass was $\rho_0 = 2.6 \text{ g/cm}^3$, the nominal diameter of glass fibres was $12 \mu\text{m}$, the nominal length of the chopped roving was 50 mm , and the nominal areal weight of the mat was $Q = 450 \text{ g/m}^2$. The mats were bonded with either a polyester powder (JMp) or a polyester emulsion (JMe) that are compatible with unsaturated polyester resin (UP), holding the fibres in position until these binders will be dissolved during the impregnation process. The applied liquids were distilled water and Ashland Aropol G235 E-4163 unsaturated polyester (UP) resin, respectively. The physical properties of the used liquids such as density (ρ), dynamic viscosity (η), surface tension (γ) together with the mean wetting contact angle (θ_{average})^{23,24} and the proportionality parameter (c) were calculated by equation (14) and are summarised in Table 1.

Liquid uptake in a micro-tensiometer

Distilled water and UP resin uptake in fibrous structures made of polyester and glass fibres were tested with a Krüss K12 micro-tensiometer.¹² Figure 3 shows the principle of the liquid absorption measurement. In the case of PET yarns, a bundle of yarn samples was placed into a Teflon measuring tube of known internal diameter and length ($D = 3 \text{ mm}$, $L = 50 \text{ mm}$) (Fig. 3(a)).

The porosity in the tube was set to be the same value (≈ 0.5) for every yarn. In the other case, a relatively small sample of the fibreglass chopped strand mats (40 mm long by 30 mm wide (B)) was hung vertically in the micro-tensiometer (Figure 3(b)). A glass beaker filled with distilled water for the yarns and UP resin for the mats approaches the vertical tube or mat sample slowly, and when the first change of weight is registered, the beaker stops, and measurement of the weight increase by absorption starts (Figure 3). The mass (m), or the absorbed liquid's height (h), can be recorded as a function of time. The measurements were carried out in a controlled environment at ambient temperature (23°C).

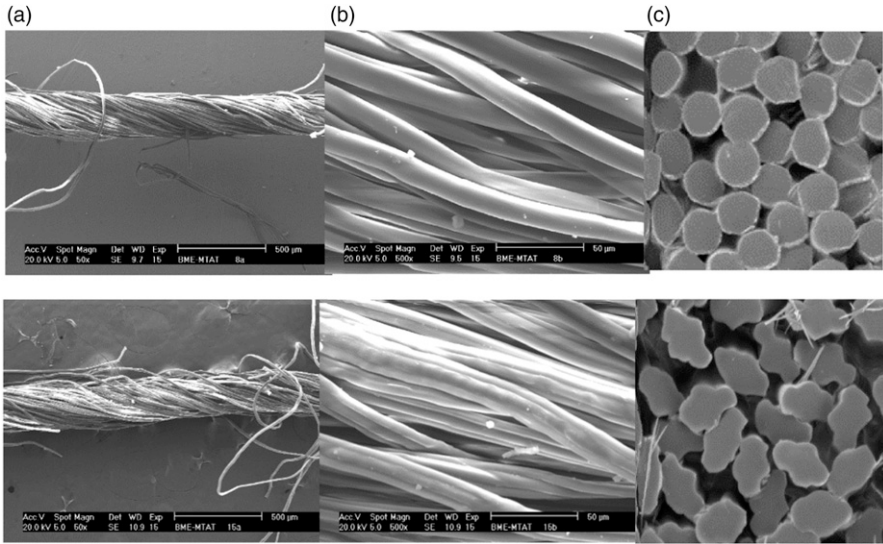


Figure 1. Longitudinal view of yarns at magnifications of 50 \times (a) and 500 \times (b) and cross-sectional images (c) of the PET fibers with round (top) and scalloped oval (bottom) cross-section based on SEM micrographs.²³

Table I. Physical parameters of the liquids and the fibre/liquid systems at ambient temperature (23°C).

Liquid and fiber	Liquid			Fiber/liquid	
	ρ (g/cm ³)	η (Pas)	γ (N/m)	$\theta_{average}$ (deg)	c (g/m)
Distilled water and PET fibre	1.00	0.001	0.0728	18	44.3
UP resin and glass fibre	1.06	0.344	0.0364	33	19.6

Results and discussion

Fitting the function by equation (20) to the measurements makes it possible to assess both the initial uptake rate (K) and the amount of liquid in steady-state (m_{∞}) and to calculate some other specific characterising parameters. Using the substitution $z = K\sqrt{t}$, the mass versus time function can be easily calculated. To fit and evaluate the yarn measurements performed with the Krüss K12 device, the same exponent parameter ($n = \sqrt{2}$) proved to be suitable in all cases in this study. Figure 4(a) shows a good correlation between approximation and experimental results ($R^2 = 0.9965$) for scalloped oval PET fibers. Since polyester is a weakly polar polymer, the measured water uptake process also includes some diffusive parts realised by water absorption driven by concentration difference; however, taking into account the large porosity in the measuring tube ($\approx 50\%$), this process was obviously dominated by the capillary part, including both the capillaries within and

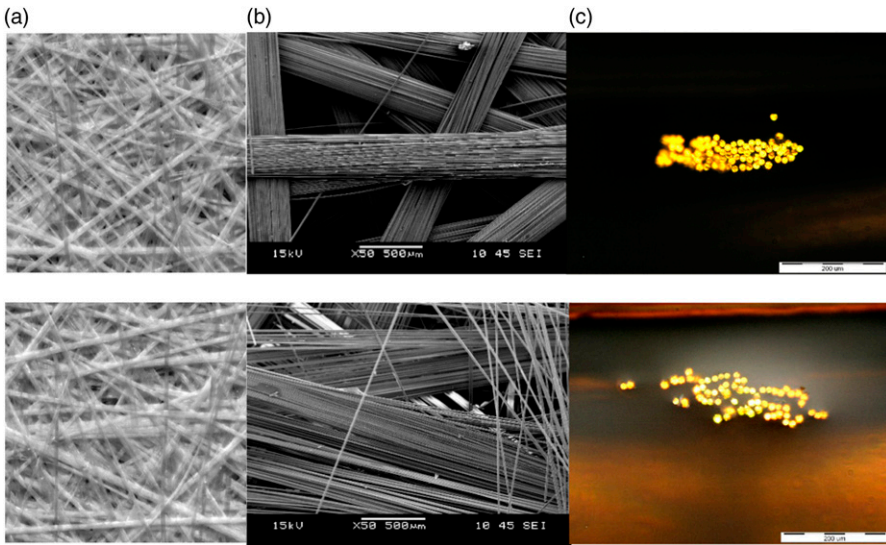


Figure 2. Optical view (a), surface images captured with SEM at magnification 500× (b) and cross-sectional view (c) of the chopped roving of glass fibre mats JM_e (top) and JM_p (bottom).²⁴

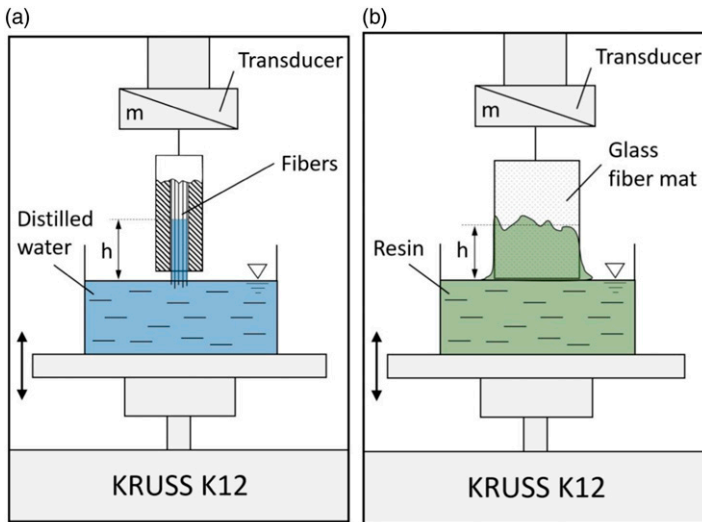


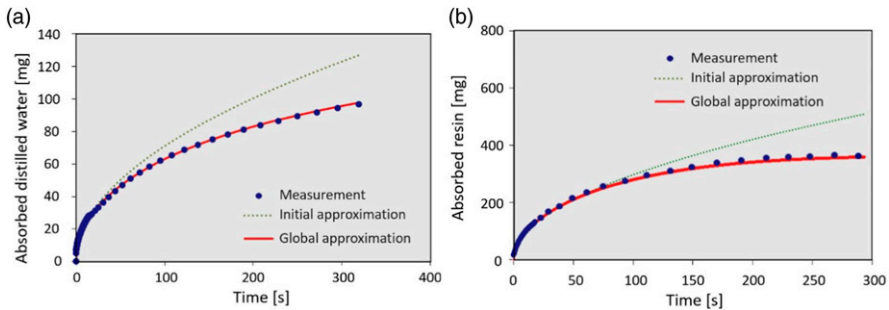
Figure 3. Schematic arrangement of liquid absorption measurement with micro-tensiometer (Krüss K12) in case of polyester yarns (a) and fiberglass chopped strand mats, CSM (b).

Table 2. Fitted and calculated parameters for water uptake of the PET yarns.

Fiber cross section	K (mg/s ^{1/2})	m_{∞} (mg)	K/m_{∞} (s ^{-1/2})	a (mg ² /s)	b (mg/s)
Round	3.1	80	0.039	4.81	0.060
Scalloped oval	5.8	147	0.040	16.82	0.114

Table 3. Fitted and calculated parameters for the resin uptake of the glass fibre mats.

Sample code	K (mgs ^{-1/2})	m_{∞} (mg)	K/m_{∞} (s ^{-1/2})	a (mg ² /s)	b (mg/s)
JMp	32.2	457	0.071	518	1.13
JMe	30.0	358	0.084	450	1.26

**Figure 4.** Typical measured, initial approximated, and global explicit approximated absorption curves for scalloped oval PET fibers (a) and for the glass fiber mat JMe (b).

between the yarns (see equation (22)). The dominant capillary action works like wicking. Fitting equations (20) to a set of measured points provides the equilibrium value (m_{∞}). The results are summarised in Table 2. According to the results related to the PET yarns in Table 2, obtained at about the same porosity in the tube, the larger amount of water (m_{∞}) was taken up by fibres with the scalloped oval cross-section (Figure 1).

Moreover, in the case of the scalloped oval fibers with a rugged enough cross-sectional shape (Figure 1), every parameter was significantly larger than for the round fibres other. This can be explained by the possibly far more capillaries between such fibres that provided higher or full water uptake in the tube filled with about the same porosity.

In the case of the fibreglass chopped strand mats, the resin uptake was taken place by capillary action between the glass fibres within the fibre tows, similar to wicking. The pores between the fibre tows are able to store the absorbed resin. The global approximation according to equation (20) was also fitted with the same exponent ($n = 3$) for each mat (Figure 4(b); $R^2 = 0.9891$), and the fitted parameters obtained are listed in Table 3. Based on the fitted (K , m_{∞}) data, it can be established that the JMp mat behaved as it had

more active capillaries of high absorption than the JMe mat, which is confirmed by the looser fibrous structure of the fibre tows within the JMp mat (Figure 2).

Disregarding the different sizes, structures, and materials of the samples, the comparison of the normalised initial intensity data (K/m_∞) in Tables 2 and 3 show that water uptake was distinctively of smaller intensity in the polyester yarns ($\leq 0.04 \text{ s}^{-1/2}$) than the resin uptake in the fiberglass chopped strand mats ($\geq 0.07 \text{ s}^{-1/2}$); however, all these values were of the same magnitude; moreover, they ranged in a rather small interval (0.03–0.09 $\text{s}^{-1/2}$).

Conclusions

Based on the variable transformations of a simple basic saturation function and their linear combination, a saturation function construction method is proposed in this paper to develop a tailored, robust approximation for fitting data obtained from finite saturation process measurements. It not only makes the retention of the measured initial behaviour possible but also allows the assessment of the saturation level. As a demonstration of the applicability of the method developed here, liquid uptake processes were analysed based on the classical Lucas-Washburn (LW) equation. The solution of the simplified LW equation has widely been used for characterising initial liquid absorption based on microtensimeter measurements. This was referred to as initial approximation ($s_0(t)$) here. The global explicit approximation as a basic NSF was derived based on the general implicit solution of the LW equation and the construction method proposed. It can easily and robustly be fitted to real liquid uptake processes, including both capillary and diffusive liquid uptake. Distilled water and UP resin absorption on polyester staple yarns and vertically positioned fiberglass chopped strand mat (CSM) samples were measured and evaluated, respectively, with Krüss K12 equipment as described earlier. The tailored saturation function obtained from applying the construction method proposed here provided a good correlation with the measured liquid uptake processes ($R^2 > 0.989$). All these results demonstrate and verify the applicability of the developed evaluation method. In addition, based on the fitted and calculated data in Tables 2 and 3 and their evaluation, it can be established that the liquid uptake tests and their evaluation method that are used here can give relevant information about the materials, such as the initial liquid uptake rate (K) and the saturation value (m_∞). Besides them, the exponent n can characterize the global liquid uptake process. The fact that this exponent was the same for the similar fibrous materials tested ($n = \sqrt{2}$ and three for yarns and mats, respectively) confirms the applicability of the tailored saturation function derived. In conclusion, with the presented method, the saturation process, and the interactions between liquid and structure, the material behavior can be characterised and distinguished.

Declaration of conflicting interests

The author(s) declared no potential conflicts of interest with respect to the research, authorship, and/or publication of this article.

Funding

The author(s) disclosed receipt of the following financial support for the research, authorship, and/or publication of this article: This research was supported by the Hungarian National Research, Development, and Innovation Office (NKFIH) through grant OTKA K116189 and it was connected to the Hungarian Ministry of Human Capacities (EMMI) for funding through the BME Nanotechnology FIKP grant (BME FIKP-NAT). The liquid absorption tests with the Krüss K12 instrument were carried out in cooperation with the Technical University of Liberec. The authors would like to thank John Summerscales, Plymouth University, for his helpful comments on the draft manuscript.

ORCID iD

Marianna Halász  <https://orcid.org/0000-0002-0289-8817>

References

1. Morton W and Hearle J. *Physical Properties of Textile Fibers*. 4th ed. Cambridge: Woodhead Publishing, 2008, pp. 202, 204, 251.
2. Krainoi A, Kummerloewe C, Nakaramontri Y, et al. Influence of carbon nanotube and ionic liquid on properties of natural rubber nanocomposites. *Express Polym Lett* 2019; 13: 327–348. DOI: [10.3144/expresspolymlett.2019.28](https://doi.org/10.3144/expresspolymlett.2019.28).
3. Zheng G, Kang Y, Sheng J, et al. Influence of moisture content and time on the mechanical behavior of polymer material. *SCI CHINA SER E* 2004; 47: 595–607. DOI: [10.1360/04ye0119](https://doi.org/10.1360/04ye0119).
4. Siakeng R, Jawaid M, Asim M, et al. Alkali treated coir/pineapple leaf fibres reinforced PLA hybrid composites: evaluation of mechanical, morphological, thermal and physical properties. *Express Polym Lett* 2020; 14/8: 717–730. DOI: [10.3144/expresspolymlett.2020.59](https://doi.org/10.3144/expresspolymlett.2020.59).
5. Kepner GR. Saturation Behavior: a general relationship described by a simple second-order differential equation. *THEOR BIOL MED MODEL* 2010; 7: 11. Article number 11. DOI: [10.1186/1742-4682-7-11](https://doi.org/10.1186/1742-4682-7-11).
6. Tu Sh-T, Cai W-Zh, Yin Y, et al. Numerical Simulation of Saturation Behavior of Physical Properties in Composites with Randomly Distributed Second-phase. *J COMPOS MATER* 2005; 39: 617–631. DOI: [10.1177/0021998305047263](https://doi.org/10.1177/0021998305047263).
7. Osenton ThG. *The Death of Demand: Finding Growth in a Saturated Global Economy*. NJ: Financial Times Prentice Hall Books, 2004.
8. Török D and Kovács JG. Effects of injection molding screw tips on polymer mixing. *Periodica Polytech Mech Eng* 2018; 62: 241–246. DOI: [10.3311/PPme.12183](https://doi.org/10.3311/PPme.12183).
9. Imre E, Bálint Á, Nagy L, et al. Examination of saturated hydraulic conductivity using grading curve functions. In: ISC'6 Conference on Geotechnical and Geophysical Site Characterisation, Budapest, Hungary, 26–29 September 2021, Budapest: Hungarian Geotechnical Society. paper no. ISC2020-373, 12 p. <http://isc6.org/images/Cikkek/Sessions/ISC2020-373.pdf>
10. Bálint Á and Mészáros Cs. Modelling of the simultaneous convection-diffusion process through porous media with percolative-fractal character at presence of anomalous diffusion. In: ICEEE-2020 11th International Annual Conference on Sustainable Environmental Protection & Waste Management Responsibility (ed Hosam, E.A.F. Bayoumi Hamuda), Budapest,

- Hungary, 19–20 November 2020, pp. 239–242. Budapest: Óbuda University. http://www.iceee.hu/downloads/11th/11th_iceee_proceedings_book.pdf
11. Mészáros Cs, Farkas I, Gottschalk K, et al. Mathematical modeling of the simultaneous convection-anomalous diffusion processes in porous media. *Drying Technology* 2017; 35: 994–998. DOI: [10.1080/07373937.2016.1274323](https://doi.org/10.1080/07373937.2016.1274323).
 12. Rulison CH. *Wettability studies for porous solids including powders and fibrous materials*. Hamburg: Krüss Technical Note, 302e, 1996, https://www.kruss-scientific.com/fileadmin/user_upload/website/literature/kruss-tn302-en.pdf
 13. Lucas R. Ueber das Zeitgesetz des kapillaren Aufstiegs von Flüssigkeiten. *Colloid Polym Sci* 1918; 23: 15–22. DOI: [10.1007/BF01461107](https://doi.org/10.1007/BF01461107).
 14. Washburn EW. The dynamics of capillary flow. *Phys Rev* 1921; 17: 273–283. DOI: [10.1103/PhysRev.17.273](https://doi.org/10.1103/PhysRev.17.273).
 15. Korn GA and Korn ThM. *Mathematical Handbook for Scientists and Engineers*. 2nd ed. New York: McGraw-Hill Book Co., 1968, Chapters 4.10.4, 4.7.2.
 16. Schoelkopf J, Gane PAC, Ridgway CJ, et al. Practical observation of deviation from lucas-washburn scaling in porous media. *Colloids Surf A: Physicochem Eng Asp* 2002; 206: 445–454. DOI: [10.1016/S0927-7757\(02\)00066-3](https://doi.org/10.1016/S0927-7757(02)00066-3).
 17. Hamraoui A and Nylander T. Analytical approach for the lucas–washburn equation. *J Colloid Interf Sci* 2002; 250: 415–421. DOI: [10.1006/jcis.2002.8288](https://doi.org/10.1006/jcis.2002.8288).
 18. Berthier J, Gosselin D and Berthier E. A generalization of the Lucas-Washburn-Rideal law to composite microchannels of arbitrary cross section. *Microfluid Nanofluid* 2015; 19: 495–507. DOI: [10.1007/s10404-014-1519-3](https://doi.org/10.1007/s10404-014-1519-3).
 19. Cai J, Jin T, Kou J, et al. Lucas–Washburn equation-based modeling of capillary-driven flow in porous systems. *Langmuir* 2021; 37: 1623–1636. DOI: [10.1021/acs.langmuir.0c03134](https://doi.org/10.1021/acs.langmuir.0c03134).
 20. Neunkirchen S, Blöbl Y and Schledjewski R. A porous capillary tube approach for textile saturation. *Compos Sci Technol* 2022: 109450. In Press. DOI: [10.1016/j.compscitech.2022.109450](https://doi.org/10.1016/j.compscitech.2022.109450).
 21. Carter HG and Kibler KG. Rapid moisture-characterization of composites and possible screening applications. *J Compos Mater* 1976; 10: 355–370. DOI: [10.1177/002199837601000408](https://doi.org/10.1177/002199837601000408).
 22. Belhadj B, Abdelkader L and Chateaufneuf A. Weibull probabilistic model of moisture concentration build up in a fiber graphite/epoxy polymer composite under varying hydrothermal conditions. *Periodica Polytech Mech Eng* 2021; 65/1: 27–37. DOI: [10.3311/PPme.13653](https://doi.org/10.3311/PPme.13653).
 23. Nagy V. *Examination and Modeling of Porosity in Polyester Twisted Fibrous Structures*. PhD Thesis. HU: Budapest University of Technology and Economics, 2006, <https://repozitorium.omikk.bme.hu/bitstream/handle/10890/467/ertekezes.pdf?sequence=1>
 24. Gombos Z. Analysis and effect of the structure of glass fiber mat on the resin uptake process and the properties of composites (in Hungarian). PhD Thesis, Budapest University of Technology and Economics, HU, 2010. <https://repozitorium.omikk.bme.hu/bitstream/handle/10890/1009/ertekezes.pdf?sequence=1>